J Physiol 588.9 (2010) pp 1647–1659

The Journal of Physiology

Ganglionic transmission in a vasomotor pathway studied *in vivo*

Bradford Bratton[1], Philip Davies[1], Wilfrid Jänig[2] and Robin McAllen[1]

[1] *Howard Florey Institute, University of Melbourne, Victoria 3010, Australia*
[2] *Christian-Albrechts-Universität, Kiel, Germany*

Intracellular recordings were made *in vivo* from 40 spontaneously active cells in the third lumbar sympathetic ganglion of urethane-anaesthetized rats. In 38/40 cells ongoing action potentials showed strong cardiac rhythmicity (93.4 ± 1.9% modulation) indicating high barosensitivity and probable muscle vasoconstrictor (MVC) function. Subthreshold excitatory postsynaptic potentials (EPSPs) showed the same pattern. The 38 barosensitive neurons fired action potentials at 2.9 ± 0.3 Hz. All action potentials were triggered by EPSPs, most of which were unitary events. Calculations indicated that <5% of action potentials were triggered by summation of otherwise subthreshold EPSPs. 'Dominant' synaptic inputs with a high safety factor were identified, confirming previous work. These were active in 24/38 cells and accounted for 32% of all action potentials; other ('secondary') inputs drove the remainder. Inputs (21 dominant, 19 secondary) attributed to single preganglionic neurons fired at 1.38 ± 0.16 Hz. An average of two to three preganglionic neurons were estimated to drive each ganglion cell's action potentials. When cells were held hyperpolarized to block spiking, a range of spontaneous EPSP amplitudes was revealed. Threshold equivalent was defined as the membrane potential value that was exceeded by spontaneous EPSPs at the same frequency as the cell's original firing rate. In 10/12 cells examined, a continuum of EPSP amplitudes overlapped threshold equivalent. Small changes in cell excitability could therefore raise or lower the percentage of preganglionic inputs triggering action potentials. The results indicate that vasoconstrictor ganglion cells *in vivo* mostly behave not as 1:1 relays, but as continuously variable gates.

(Received 22 November 2009; accepted after revision 15 March 2010; first published online 22 March 2010)
Corresponding author R. McAllen: Howard Florey Institute, University of Melbourne, Parkville, Victoria 3010, Australia. Email: rmca@florey.edu.au

Abbreviations ANP, atrial natriuretic peptide; AP, action potentials; CR, cardiac rhythmicity; CVC, cutaneous vasoconstrictor; LST, lumbar sympathetic trunk; MVC, muscle vasoconstrictor; RMP, resting membrane potential; SCG, superior cervical ganglion.

Introduction

Sympathetic ganglion cells in the paravertebral chain receive the final neural synapse between the central nervous system (CNS) and targets such as blood vessels, sweat glands and piloerector muscles. Current accounts of their function suggest that for the most part they passively relay synaptic inputs from preganglionic neurons (Jänig, 2006). In this view, the functional contribution of the ganglionic synapse is restricted to distributing signals received from a limited number of preganglionic neurons to a large number of peripheral targets. By contrast with prevertebral ganglion cells innervating the gut (Jänig, 2006), paravertebral (including most vasomotor) ganglion cells are considered to play little integrative role. The data upon which these views are based, however, are almost entirely indirect. Very few studies have yet examined how ganglion cells integrate natural synaptic activity *in vivo* (Skok & Ivanov, 1983; Ivanov & Purves, 1989; Tatarchenko *et al.* 1990; Ivanov, 1991; Ivanov & Skok, 1992; McLachlan *et al.* 1997, 1998).

Previous studies examining synaptic processing by sympathetic ganglion cells have found that their function differs from the 'integrate-and-fire' arrangement of most central neurons. Action potentials in ganglion cells are driven mostly by unitary rather than summed EPSPs (McLachlan *et al.* 1997). Each ganglion cell receives a 'dominant' or 'strong' (always suprathreshold) synaptic

DOI: 10.1113/jphysiol.2009.185025

input from one presynaptic fibre (occasionally two) as well as a limited number of weaker synaptic inputs – the '$n+1$ rule' (McLachlan *et al.* 1998; Karila & Horn, 2000; Wheeler *et al.* 2004). Dominant synaptic inputs show several characteristics that are qualitatively distinct from other inputs (Skok & Ivanov, 1983), including dependence upon different presynaptic calcium currents (Ireland *et al.* 1999). The consequences of the $n+1$ arrangement for ganglionic function *in vivo* are not yet understood.

The most comprehensive previous examination of sympathetic ganglion cell function *in vivo* studied superior cervical ganglion (SCG) neurons (McLachlan *et al.* 1997, 1998). In those studies, impaled cells were held slightly hyperpolarized by steady current injection (holding potential ~ -60 mV (McLachlan *et al.* 1997, 1998)). Hyperpolarization to this level did not block action potentials triggered by dominant EPSPs (McLachlan *et al.* 1998), but would have de-emphasized the role played by other synaptic inputs. The functional role played by those other inputs remains unclear.

A further issue requiring clarification stems from the fact that previous studies of this nature have focused on SCG cells, which are functionally heterogeneous (Li & Horn, 2006; Cane & Anderson, 2009). Much evidence supports the view that ganglion cells of each sympathetic functional class have distinct phenotypes and characteristic properties (Horn & Stofer, 1989; Jänig & McLachlan, 1992). In the analyses by McLachlan *et al.* (1997, 1998), 5/11 neurons studied in detail were shown to possess moderate cardiac rhythmicity (51–77%), indicating that they were barosensitive and thus probably vasomotor to tissues in the head. It would be of value to extend the analysis of synaptic processing of natural EPSPs (as opposed to those generated by synchronous activation of preganglionic fibres by electrical stimuli) to a larger, clearly defined vasomotor cell population. We therefore set out to study ongoing synaptic events occurring *in vivo* in a more restricted population of neurons that mostly supply blood vessels in the hindlimb.

Methods

General procedures

All experiments were performed in accordance with the Australian National Health and Medical Research Council code of practice for the care and use of animals for scientific purposes and were approved by the Animal Experimentation Ethics Committee of the Howard Florey Institute. The experiments were performed on 17 male Sprague–Dawley rats (263–570 g body weight). Rats were sedated with sodium pentobarbitone (45 mg kg^{-1} I.P.) then anaesthetized with 2% isofluorane throughout the surgical preparation. For the experiment, isofluorane anaesthesia was withdrawn gradually over 30 min and replaced over that time by urethane (1–1.5 g kg^{-1} I.V.). Anaesthesia was then maintained at a depth sufficient to suppress corneal and withdrawal reflexes, by supplementary doses of urethane (0.125 g kg^{-1} I.V.). No neuromuscular relaxant was given.

Rats were artificially ventilated (2.8 ml, 70 strokes min^{-1}) with oxygen through a tracheostomy. Ventilation was adjusted to suppresss spontaneous respiratory movements and to maintain end tidal CO_2 levels near 4%. The right femoral artery and vein were cannulated in order to record blood pressure (108 ± 2.7 mmHg) and for drug delivery, respectively. Body temperature was maintained near 37°C by a feedback-controlled heating blanket linked to a rectal thermistor probe (FHC Frederick Haer & Co. Bowdoin, ME, USA). The left lumbar sympathetic trunk (LST) was exposed using a lateral retroperitoneal approach. The LST was cut just proximal to the L4 ganglion. The proximal part of the LST, including the L3 ganglion, was cut free from surrounding tissue and mobilized as far rostrally as the L2 ganglion, whose neural and vascular connections were preserved. The L3 ganglion remained attached to its proximal neural connections. Approximately 8 mm of free LST connected the L3 ganglion to its proximal tethering point. A 32×20 mm vessel (vol. 6 ml) was placed into the abdominal cavity containing a separately supported rigid 7 mm diameter silicone-elastomer covered platform (Sylgard, Dow-Corning, Midland, MI, USA). The L3 ganglion was pinned out on this platform with fine 25 μm diameter tungsten pins and bathed with warmed Krebs–Henseleit buffer (composition in mM: 118 NaCl, 5.4 KCl, 1.0 $MgSO_4$, 1.9 $CaCl_2$, 1.0 NaH_2PO_4, 25 $NaHCO_3$, and 11.1 dextrose) saturated with carbogen (95% O_2–5% CO_2) and maintained at 37 ± 1°C. The rear opening to the chamber (nerve entrance) was sealed with Kwik-Cast silicone elastomer sealant (WPI, Sarasota, FL, USA) to block fluid movements. The connective tissue sheath covering the pinned ganglion was partially removed using fine forceps and pins.

Cardiac rhythmicity (CR) of action potentials (APs) and subthreshold EPSP events were determined by pulse-triggered histograms of synaptic or AP events, using a bin size of 10 ms and a window of 300 ms before and after the triggering pulse wave. The trigger pulse was taken from the systolic peak, and at least 100 triggers were used to construct each histogram. The arterial pulse wave was averaged with respect to the same trigger times. To quantify cardiac rhythmicity, the mean difference between the histogram peak and nadir was expressed as a percentage of the peak (cf. Boczek-Funcke *et al.* 1992).

Intracellular recordings

Intracellular recordings of spontaneous activity in lumbar sympathetic ganglion cells with intact central connections

were made, using sharp KCl filled microelectrodes (0.5 M, tip resistance 70–130 MΩ) to impale ganglion cells. After impalement, cells were allowed to stabilize for 1–5 min before data collection. Data were acquired by a CED Power-1400 mark II data acquisition system (Cambridge Electronic Design Ltd, Cambridge, UK), using 10 kHz sampling frequency (16 bit precision) for voltage and current recordings and 200 Hz for blood pressure, temperature, respiratory pressure and end-expiratory CO_2 levels. Digitized data were stored on a computer and analysed off line. Recordings of action potentials and synaptic activity were made in bridge mode with an Axoprobe 2B amplifier (Axon Instruments, Union City, CA, USA). The bridge was balanced and capacitance compensation used in all experiments. Passive membrane properties (membrane resistance and capacitance) were determined at intervals during the impalement from the voltage transient evoked in response to small hyperpolarizing current steps (0.5 nA, 100 ms duration, 0.1 Hz). For periods during the recording, the cell was hyperpolarized from resting membrane potential (RMP) to between −80 and −150 mV in order to block action potentials and to determine characteristics of the underlining EPSP activity.

At the end of the experiments animals were killed with sodium pentobarbitone (120 mg kg^{-1} I.V., Lethabarb, Virbac, Australia).

Statistics and presentation

All values are presented as means ± standard error of mean and ranges unless stated otherwise. Recordings were made from 61 lumbar sympathetic ganglion cells with spontaneous activity. Of these, 40 were selected for analysis on the following criteria: resting membrane potential of at least −35 mV; action potential that crossed zero mV; stable recording held for at least 2 min. Data acquisition and analysis were performed using the general purpose capture and analysis package Spike II (Cambridge Electronic Design).

Results

Ganglion cells with ongoing activity were selected for study. Stable impalements lasting between 2 and 150 min were made from 40 active ganglion cells with resting membrane potentials of −49.9 ± 1.2 mV (range −36.0 to −67.0 mV) and action potential amplitudes 71 ± 2 mV (range 45.0 to 93.8 mV). Cell input resistance was 91.4 ± 11.5 MΩ and membrane time constant 5.5 ± 0.6 ms (26 cells).

Ongoing activity in ganglion cells consisted in all cases of action potentials (rate 2.9 ± 0.3 Hz) and in most cases (36/40) also of subthreshold EPSPs (rate 2.6 ± 0.4 Hz) see Fig. 1*A*. No hyperpolarizing synaptic potentials were

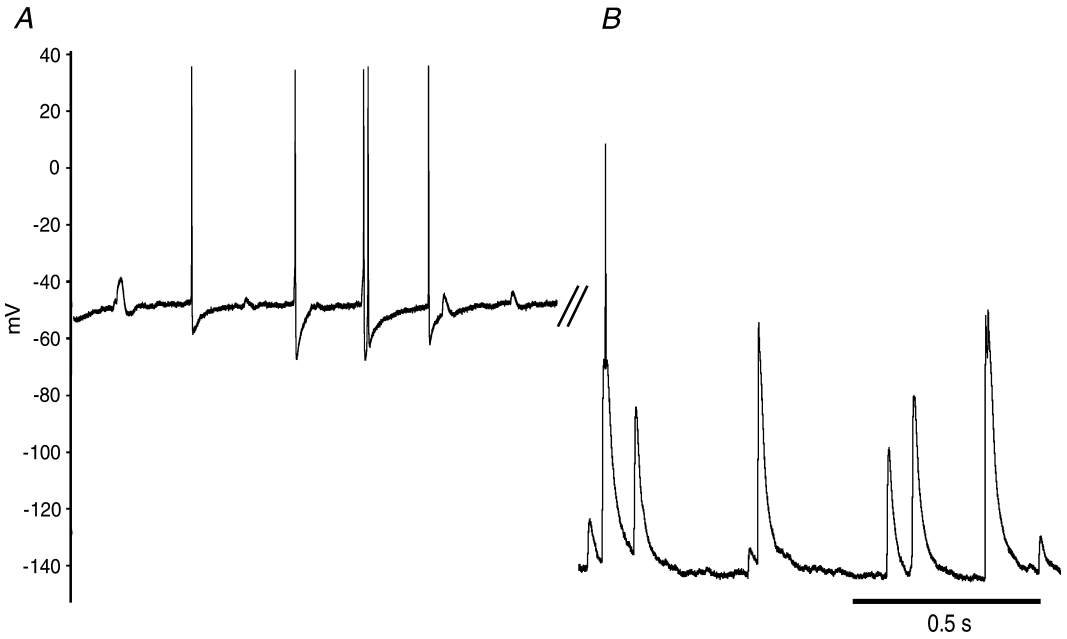

Figure 1. Ongoing activity in ganglion cells
A, action potentials and subthreshold EPSPs recorded at resting membrane potential (−47 mV). *B*, record from the same cell while membrane potential was hyperpolarized to −140 mV. Note the range of EPSP amplitudes. Most but not all action potentials were blocked by this degree of hyperpolarization (see the spike remainder riding on the EPSP second from left).

detected. Subthreshold EPSPs ranged in amplitude within and between cells, from the noise level up to ∼15 mV. Hyperpolarizing cells to block action potentials revealed the synaptic potentials that were responsible for this ongoing activity (Fig. 1*B*).

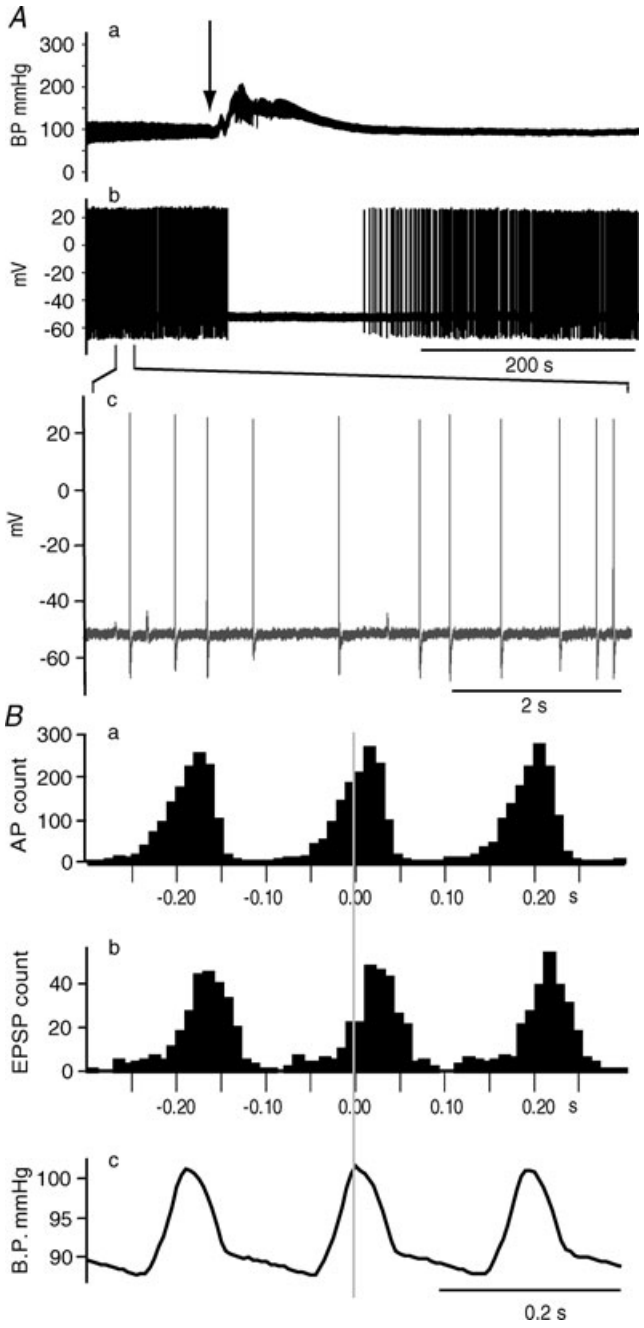

Figure 2. Barosensitivity of ganglion cells
A, ongoing activity of a ganglion cell (*b*), showing that it was inhibited during the period of increased blood pressure (*a*) after 1.2 μg phenylephrine was injected I.V. (at arrow). Inset (*c*) is an expanded section from *b* to show the presence of subthreshold EPSPs as well as action potentials. *B*, cardiac cycle-triggered histograms of ongoing spike activity (*a*) and subthreshold EPSPs (*b*). The trigger time is shown as a vertical line in the averaged arterial pulse waveform (*c*). 1409 triggers were used to generate the histograms.

Functional class of neurons

Cardiac cycle-triggered histograms were constructed from ongoing spike activity, and these showed cardiac modulation in 38/40 cells. The degree of cardiac modulation of those 38 cells was very strong (mean $93.4 \pm 1.9\%$), indicating high barosensitivity (see also Fig. 2*A*). The subthreshold EPSPs present in those cells also showed strong cardiac modulation (Fig. 2*Bb*). One of the neurons without cardiac rhythmicity had subthreshold EPSPs, and these also lacked cardiac rhythmicity (not shown). Data from the two cells lacking cardiac rhythmicity were excluded from further analysis.

Basis of ongoing activity

To study the synaptic basis of ongoing activity in these cells, they were hyperpolarized by steady current injection. Twelve cells selected for detailed analysis were hyperpolarized to between −80 and −150 mV. Confirming previous observations on SCG neurons (McLachlan *et al.* 1997, 1998) it was usually (though not always) possible to block action potentials. EPSP shapes indicated that most were unitary events (Figs 1*B* and 4) triggered by single preganglionic action potentials. On occasion, however, subthreshold EPSPs coincided and summed (Fig. 4*A*), presumably when preganglionic action potentials from two sources arrived within a brief interval. To estimate the contribution of such EPSP summation to ganglion cell spike activity, synaptic events in the hyperpolarized cell were examined in parallel records of membrane potential and its first derivative (dV/dt, Fig. 4*A*, lower trace). The dV/dt trace satisfactorily resolved individual synaptic inputs, picking out the differences in slope when two or more EPSPs summed (Fig. 4*A*, event *a*).

The frequency of action potentials in the cell was measured before it was hyperpolarized, and this value could be used to estimate the 'threshold equivalent' in the hyperpolarized voltage record (Fig. 3*A*). Threshold equivalent was defined as the level of membrane potential that was crossed by spontaneous EPSPs at the same frequency as the cell's original firing rate. For further explanation, see the diagram in Fig. 3. Assuming that synaptic inputs were unchanged and that EPSP amplitude reflects synaptic strength, EPSPs that failed to reach threshold equivalent would have been subthreshold, while those that exceeded threshold equivalent would have triggered action potentials in the undisturbed cell.

Next, using the close relation between the amplitude and peak dV/dt for unitary EPSPs (Fig. 4*B*), a 'unitary threshold equivalent' could be drawn on the dV/dt trace (Fig. 4*A*, lower trace). Unitary threshold equivalent was set by interpolation between the peak dV/dt values of unitary EPSPs just reaching, and those just failing to reach, threshold equivalent on the voltage trace. Cases where the

summed EPSPs reached threshold equivalent in the voltage trace but failed to reach unitary threshold equivalent in the dV/dt (e.g. Fig. 4*A*, event *a*) trace were taken to show summation to threshold by otherwise subthreshold events. The incidence of such events was measured and compared with the firing rate of the cell.

In 10/12 selected ganglion cell recordings, the percentage of action potentials attributable to EPSP summation was low (range 0–3.3%), but in the remaining two cells it was 17.3 and 18.3%: overall, the mean incidence was 4.2 ± 1.9%. Summation of subthreshold EPSPs contributed 0.11 Hz (3.5%) to the mean firing rate of 3.1 Hz in the 12 cells.

Two types of suprathreshold synaptic input

Confirming previous observations on sympathetic neurons (Purves, 1975; Skok & Ivanov, 1983; Horn & Stofer, 1988; McLachlan *et al.* 1997, 1998; Karila & Horn, 2000), we found that two types of action potential profile could be identified in lumbar ganglion cells. Dominant inputs triggered action potentials (labelled '1' in Fig. 5*A–D*) with a very rapid initial depolarization (mean rate of depolarization between 5 and 10 mV above resting membrane potential (19 ± 1.4 V s^{-1}, $n = 24$) and usually a small afterhyperpolarization. Other inputs (called 'accessory' by Skok & Ivanov (1983), but here referred to as 'secondary' (cf. Karila & Horn, 2000) triggered action potentials with slower initial depolarizations and usually larger afterhyperpolarizations (labelled '2' in Fig. 5*A–D*). The profiles of action potentials driven by the two types of input were most readily distinguished in phase-plane plots (Fig. 5*D*).

Spontaneous action potentials driven by dominant inputs were present in 24/38 cells (cells with open or grey columns in Fig. 6), and those driven by secondary inputs in 37 cells (cells with black columns in Fig. 6). Thus, spontaneous action potentials were driven by both dominant and secondary synaptic inputs in 23 cells, by secondary synaptic inputs only in 14 cells, and by a dominant synaptic input only in one cell. In the population of cells where they were present, dominant inputs drove action potentials at 1.37 ± 0.17 Hz, accounting for 39% of those 24 cells' spike activity. The full population of 38 cells fired at 2.9 ± 0.3 Hz, and dominant synaptic inputs accounted for 32% of this (Fig. 6).

Numbers of preganglionic inputs driving action potentials in each cell

In each cell, action potentials of each type were sorted by spike shape, with additional reference to phase-plane plots. The time sequences of these separated action potentials were then subjected to autocorrelation analysis (Perkel *et al.* 1967). Figure 5*C* illustrates the process. When all action potentials were included, the autocorrelogram showed no central gap (Fig. 5*C*, upper trace). This reflects the fact that the refractory period of the ganglion cell itself was less than the 10 ms bin size, allowing the occurrence of short interspike intervals that filled the central bins. When the spike trains of the two types were discriminated and separated, however, both individually gave autocorrellograms with a gap of ~200 ms either side of the central trigger time (Fig. 5*C*, middle traces). The activity of single sympathetic preganglionic neurons *in vivo* is characterized by a lack of short interspike intervals (Polosa *et al.* 1982; Kubota *et al.* 1995); we therefore interpret this pattern as showing that each separated spike train was driven by a single preganglionic neuron. Autocorrelograms without a prominent central gap were taken to indicate that more than one preganglionic neuron was driving the activity.

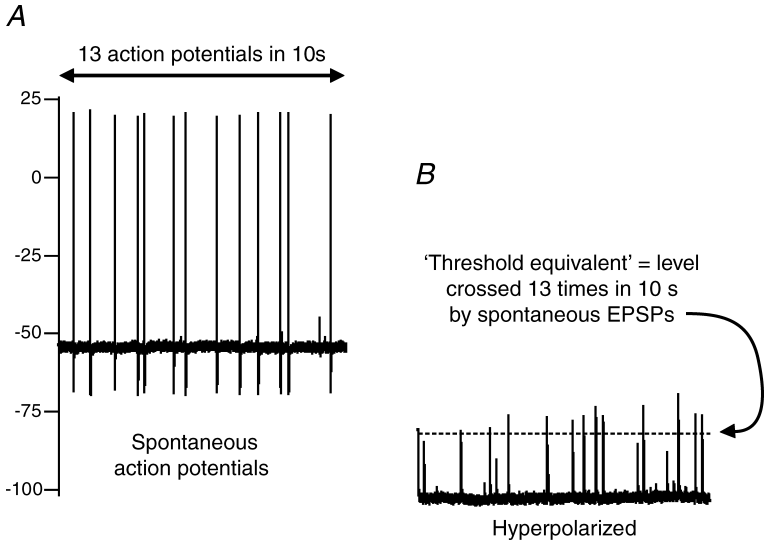

Figure 3. Derivation of threshold equivalent
Two sections of voltage record from the same cell. *A*, spontaneous firing (in this case at 1.3 Hz). *B*, same cell, membrane hyperpolarized to ~ −100 mV to block spiking and reveal EPSPs. 'Threshold equivalent' in this case is the level crossed at 1.3 Hz by spontaneous EPSPs.

This analysis indicated that for 21 ganglion cells, a single preganglionic neuron provided the dominant input. For three other cells (indicated in Fig. 6 by asterisks), dominant inputs came from at least two preganglionic neurons. Nineteen ganglion cells received a suprathreshold secondary input from a single preganglionic neuron, while a further 18 ganglion cells received such inputs from two or more preganglionic neurons. Six cells (e.g. the cell shown in Fig. 5) received both a single dominant and a single secondary input. While APs in most ganglion cells were driven from more than one source, a single preganglionic neuron drove the activity of 8/38 cells. That input was dominant in only one case.

The mean firing rate of unitary dominant inputs driving action potentials was 1.23 ± 0.17 Hz ($n = 21$) and for suprathreshold secondary inputs was 1.54 ± 0.29 Hz ($n = 19$). The overall mean firing rate of unitary preganglionic inputs driving action potentials was 1.38 ± 0.16 Hz ($n = 40$), and their distribution is shown in Fig. 7.

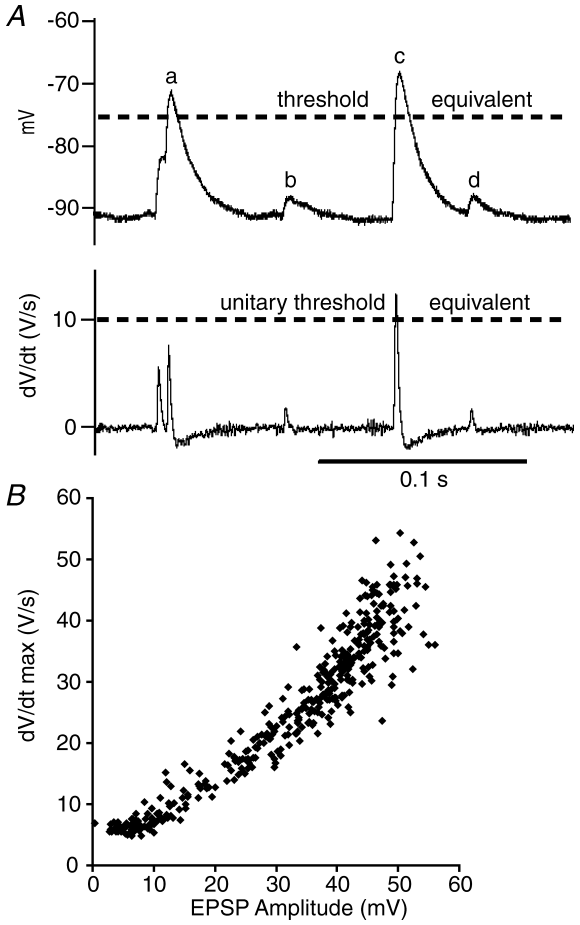

Figure 4. Method used to determine the incidence with which otherwise subthreshold EPSPs summed to reach threshold
A, upper trace, an intracellular recording from a ganglion cell hyperpolarized to −90 mV by constant current injection. Lower trace, the corresponding record of the first derivative of membrane potential (d*V*/d*t*). Unitary synaptic events may be seen as distinct deflections in the d*V*/d*t* trace, identifying which EPSPs were unitary (e.g. events labelled *b*, *c* and *d*) and which were summed (e.g. the event labelled *a*). Threshold equivalent (see Fig. 3 and text) is shown by the horizontal dashed line in the upper trace. Unitary threshold equivalent is shown by the horizontal dashed line in the lower trace; it was derived by interpolation between the d*V*/d*t* values of unitary events that just reached and those that just failed to reach threshold equivalent on the voltage trace. *B* shows, for another cell, the close relation that links the amplitude of unitary EPSPs and their maximum rate of depolarization.

Analysis of EPSP amplitudes

The 12 cells selected for detailed analysis were hyperpolarized to between −80 and −150 mV by steady current injection. Dominant synaptic inputs were present in eight of these cells, and could be recognized as the largest unitary EPSPs. Their amplitudes (excluding 'mini-spikes' that persist atop some of the largest EPSPs, see Fig. 1*B* and McLachlan *et al.* 1998) measured from the hyperpolarized holding potential ranged from 27 to 90 mV in different cells. Because hyperpolarization increases the driving potential that generates EPSPs, those values exaggerate the true picture. They were therefore transposed back to their notional amplitudes at resting membrane potential (-54 ± 3 mV), on the basis that the ion currents generating nicotinic EPSPs reverse at ∼0 mV (Yawo, 1989; Selyanko *et al.* 1995). The calculated amplitudes of dominant EPSPs at resting membrane potential were 28.5 ± 3 mV (range 15–40 mV, $n = 8$).

A further analysis was performed on the distribution of amplitudes of all EPSPs in those 12 cells, and their relation to threshold equivalent. For each cell, the cumulative frequency (ordinate) of EPSPs exceeding a given amplitude (abscissa) was plotted as shown in Fig. 8*C*. The resting firing rate of the cell before hyperpolarization was measured (Fig. 8*A*), and this value was used to determine the threshold equivalent as described above under *Basis of ongoing activity* (Figs 4 and 8*B*). By definition, threshold equivalent (Fig. 8*C*, vertical dashed line) intersected the cumulative frequency plot at the cell's original firing rate (3.6 Hz in this case). In two cases (Fig. 9*F* and *H*) the threshold equivalent intersected the cumulative frequency plot close to a plateau, indicating that almost all EPSPs were either clearly sub- or suprathreshold. In cells such as these, firing rate would change little if cell threshold were shifted by a few millivolts. In the remaining 10 neurons, however, threshold equivalent intersected a sloping section of the plot. From this we can infer that the incoming EPSPs in those cells had a range of amplitudes that straddled threshold. Any small change in the excitability of cells such as these (e.g. by changes in threshold, membrane potential or cell resistance) would decrease or increase the proportion of threshold-straddling EPSPs that went on to

trigger action potentials: this would alter postganglionic nerve activity in a continuously graded fashion.

Discussion

The present findings show how presumed vasoconstrictor ganglion cells process their natural preganglionic inputs and thus determine vasomotor tone. They extend previous findings on SCG cells – a functionally mixed population – and for the first time reveal the functional significance of two types of preganglionic input. In doing so, they indicate that vasomotor ganglion cells have the capacity to act not just as a passive relay of incoming signals, but as a continuously variable gate, where ganglionic throughput is poised to be modulated up or down by synaptic, local or circulating factors that influence cell excitability. These issues are discussed further below.

Functional identity of lumbar ganglion cells recorded

This study has focused on neurons in the third lumbar ganglion, a major source of projections to the hindlimb (Baron *et al.* 1988). The innervation targets of these ganglion cells include blood vessels in muscle and skin, sweat glands in the paw pad and piloerector muscles. Neurons supplying the sweat glands and piloerector muscles are unlikely to have been active in deeply anaesthetized animals (Grosse & Jänig, 1976; Jänig & Kümmel, 1981; Jänig & McLachlan, 1992). Rats were kept at core temperatures close to 37°C, which is near

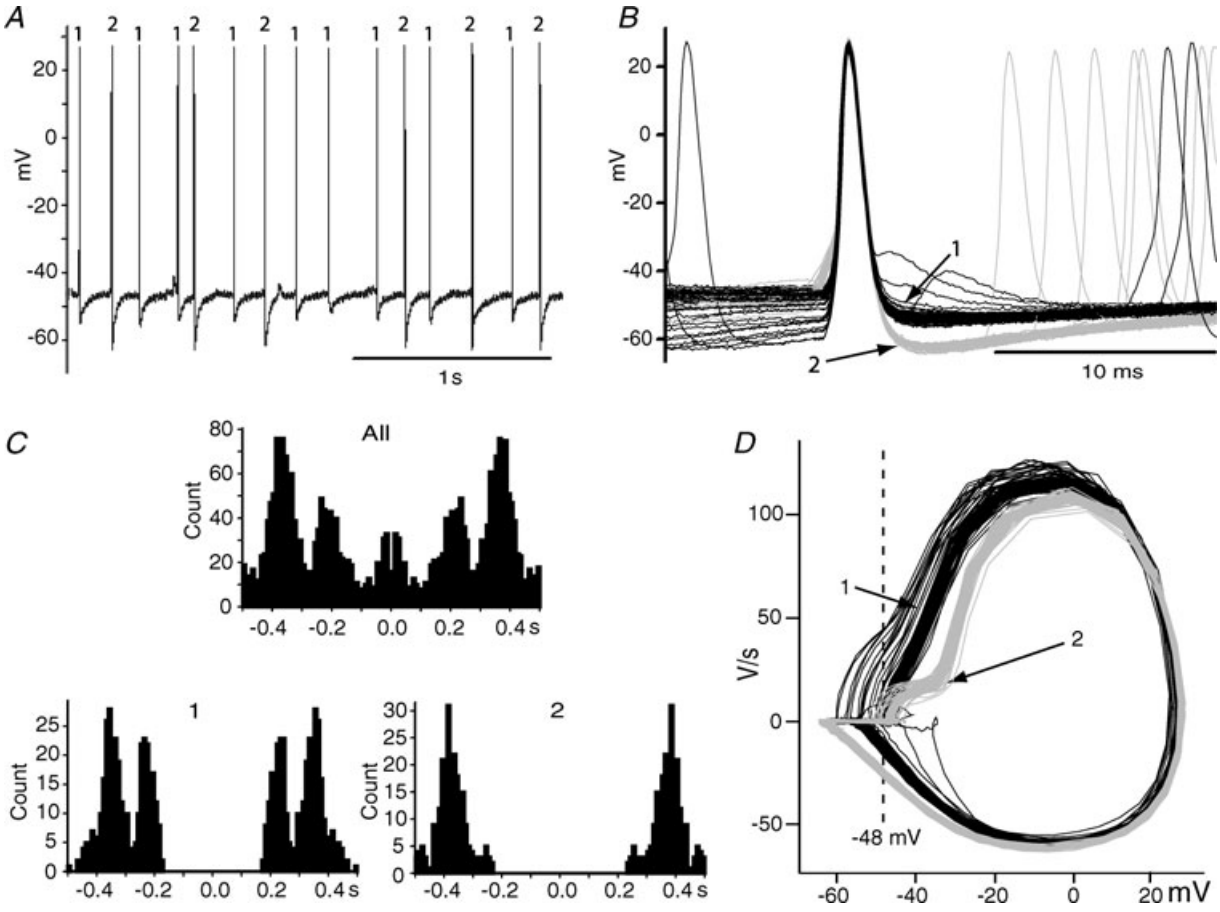

Figure 5. Two types of action potential driven by two types of synaptic input
Data shown here are taken from a single cell that received one dominant and one secondary suprathreshold input. Action potentials driven by the dominant input (labelled '1') are distinguishable individually in the chart record (*A*) and in the superimposed spike display (*B*) by their smaller afterhyperpolarization than action potentials driven by the secondary input (labelled '2'). Less obvious in those records, but clearly shown in the phase-plane plots (*D*), is the more abrupt initial depolarization of action potentials driven by the dominant input (1). Autocorrelation analysis (*C*) showed that when all action potentials were included, the histogram contained no central gap around the trigger spike (*C*, upper record), the minimum interval between successive spikes (corresponding to the refractory period of the ganglion cell) being less than the 10 ms bin width. When the spike trains of each type were separated, however, their autocorrelograms both showed a central gap ~200 ms on either side of the trigger spike (*C*, lower records). This reflects the long refractory period of single preganglionic neurons. For further details, see text.

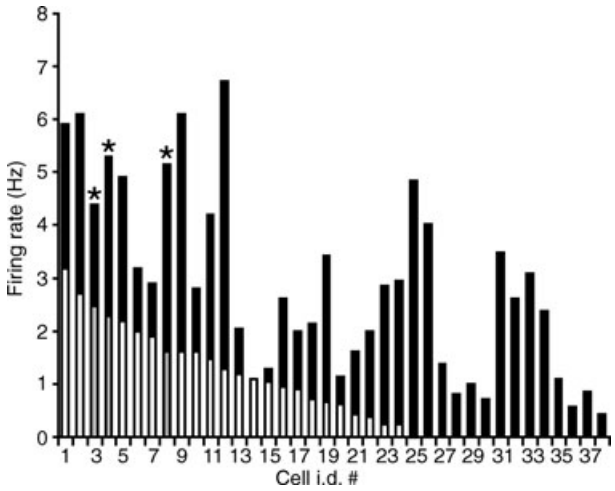

Figure 6. Firing rates of individual ganglion cells due to dominant and secondary inputs
Data from 38 barosensitive ganglion cells are presented in descending order of firing rates due to dominant inputs (white and grey columns). Rates due to secondary inputs are shown by the superimposed black columns. In the 3 cases marked by asterisks and grey bars, more than one dominant input was present. Overall, dominant inputs triggered 32% of action potentials in the population.

the threshold for activation of cutaneous vasoconstrictor (CVC) neurons supplying the hairy skin of the back (Tanaka *et al.* 2007). It is conceivable that CVC neurons supplying the leg and the foot might have lower thermal thresholds, in which case they could have had some tonic activity in the present experiments. While CVC neurons may show cardiac rhythmicity, it is rarely of the strength seen in muscle vasoconstrictor (MVC) neurons (Häbler *et al.* 1994; Jänig, 2006). MVC neurons in rats (Häbler *et al.* 1994), as in cats (Jänig, 1988) and humans (Macefield *et al.* 1994), fire less than once per heartbeat, but their firing is restricted to a limited part of the cardiac

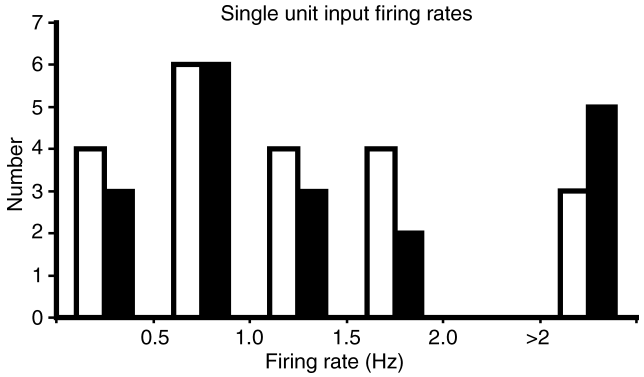

Figure 7. Firing rate distribution of unitary preganglionic inputs
This histogram shows the distribution of firing rates of suprathreshold preganglionic inputs that could be demonstrated by the methods shown in Fig. 4 to come from unitary preganglionic sources. Data from unitary dominant inputs are shown by open columns while those from secondary inputs are shown by filled columns.

cycle by the powerful phasic action of baroreceptors. The very strong cardiac modulation of the 38 neurons studied in detail here indicates that they were vasoconstrictor, probably MVC neurons. The two cells without cardiac modulation may have been CVC or other neuron types.

Comparison with previous work

The present findings show that lumbar ganglion cells with presumed vasoconstrictor function receive synaptic inputs of a size and frequency range comparable to the SCG neurons studied previously *in vivo* (McLachlan *et al.* 1997). A major difference from previous work was the much stronger cardiac rhythmicity seen in the lumbar ganglion cells recorded here (mean 93% compared with 51–77% measured in five SCG cells by McLachlan *et al.* (1997)). It seems probable that we studied a functionally different cell population from the SCG cells of McLachlan *et al.* (1997). This conclusion is supported by the lower mean cell capacitance measured here compared with that in SCG cells (75 ± 9 *vs.* 107 ± 8 pF; (McLachlan *et al.* 1997)), indicating that the lumbar ganglion cells were smaller. In keeping with this, vasoconstrictor neurons (identified *in vitro* in SCG by their properties and by their expression of neuropeptide Y) are smaller cells than those of other sympathetic classes (Li & Horn, 2006).

McLachlan *et al.* (1997) proposed that summation of subthreshold EPSPs played a minimal role in determining postganglionic spike activity, even when the system was driven hard by reflexes. In the present study we analysed this issue quantitatively for lumbar ganglion cells under basal conditions, and confirmed that in most cases the contribution of summation to ongoing spike activity was small. While imperfect cell impalements could have led to leak currents reducing membrane time constant, and hence the probability of EPSP summation, we made our measurements only after recordings had stabilized and the cell appeared to be well sealed around the electrode. We therefore do not believe that the underestimate was major. How far the contribution of summed EPSPs might increase under strong reflex stimulation (as predicted by Karila & Horn, 2000), perhaps affecting specific subsets of cells (e.g. 2/12 studied here), remains to be determined. A corollary point is that both the studies of McLachlan and colleagues (1997, 1998) and the present study refute the notion of Skok that secondary spikes are the result of summed subthreshold EPSPs (Skok & Ivanov, 1983). It is now quite clear that most action potentials of all types are driven by unitary EPSPs.

Roles of dominant and secondary synaptic inputs

The present experiments confirmed expectations that most ganglion cells receive a single dominant input that

virtually always triggers action potentials. We found such inputs to be active in 24/38 ganglion cells. While it is possible that the remaining 14 neurons did not possess any dominant input, previous studies using electrical stimuli have found that essentially all sympathetic ganglion cells receive at least one dominant input (Purves *et al.* 1986; Li & Horn, 2006). We therefore consider it most likely that the dominant input to those cells was present but silent. Strikingly, we found that most postganglionic spike activity was attributable to secondary synaptic inputs. This contradicts the prevailing view (McLachlan, 2003; Jänig, 2006) that nearly all ganglion cell action potentials are due to dominant inputs.

We now propose the following alternative view. Dominant synaptic inputs may be seen as providing obligatory transmission, where the ganglion cell acts as a simple relay with a high safety factor. Secondary inputs, with EPSPs around threshold, may be regarded as the substrate for variable transmission. Two factors, high quantal variability (Karila & Horn, 2000; Wheeler *et al.* 2004) and the presence of inputs from more than one preganglionic source, are likely to explain the broad range of EPSP amplitudes seen in these cells. As our analysis has found, this broad range usually stretches from below to above threshold equivalent in a continuous gradation. To the extent that threshold equivalent accurately predicts threshold (see below), it follows that the probability that an EPSP in this intermediate range triggers an action potential will be strongly influenced by small changes in ganglion cell threshold. In the present experiments, two-thirds of resting postganglionic activity were a result of this variable type of transmission.

For simplicity, threshold equivalent was measured here without taking account of post-AP refractoriness.

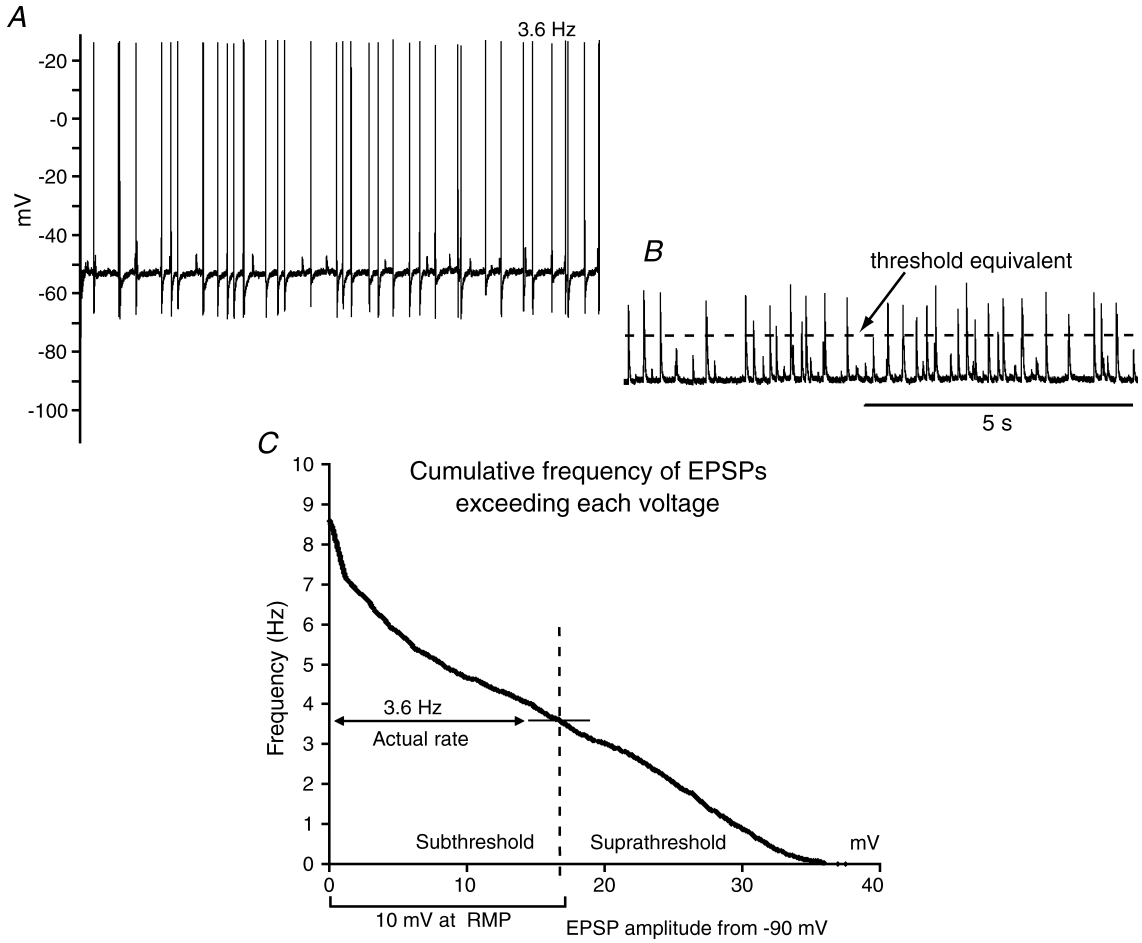

Figure 8. Analysis of EPSP amplitudes in relation to threshold equivalent
A, spontaneous activity of a cell firing action potentials at 3.6 Hz. *B*, the same cell hyperpolarized to −90 mV by steady current injection, showing spontaneous EPSPs with a range of amplitudes. The horizontal dashed line shows threshold equivalent. *C*, the cumulative frequency (ordinate, Hz) of EPSPs recorded from a baseline of −90 mV, whose amplitudes exceeded each voltage specified on the abscissa. Threshold equivalent is indicated by the vertical dashed line and the cell's original firing rate by the horizontal arrow. The amplitudes that those EPSPs would have attained from the cell's RMP (−53 mV in this case) are indicated by the 10 mV calibration bracket below. Further details in text.

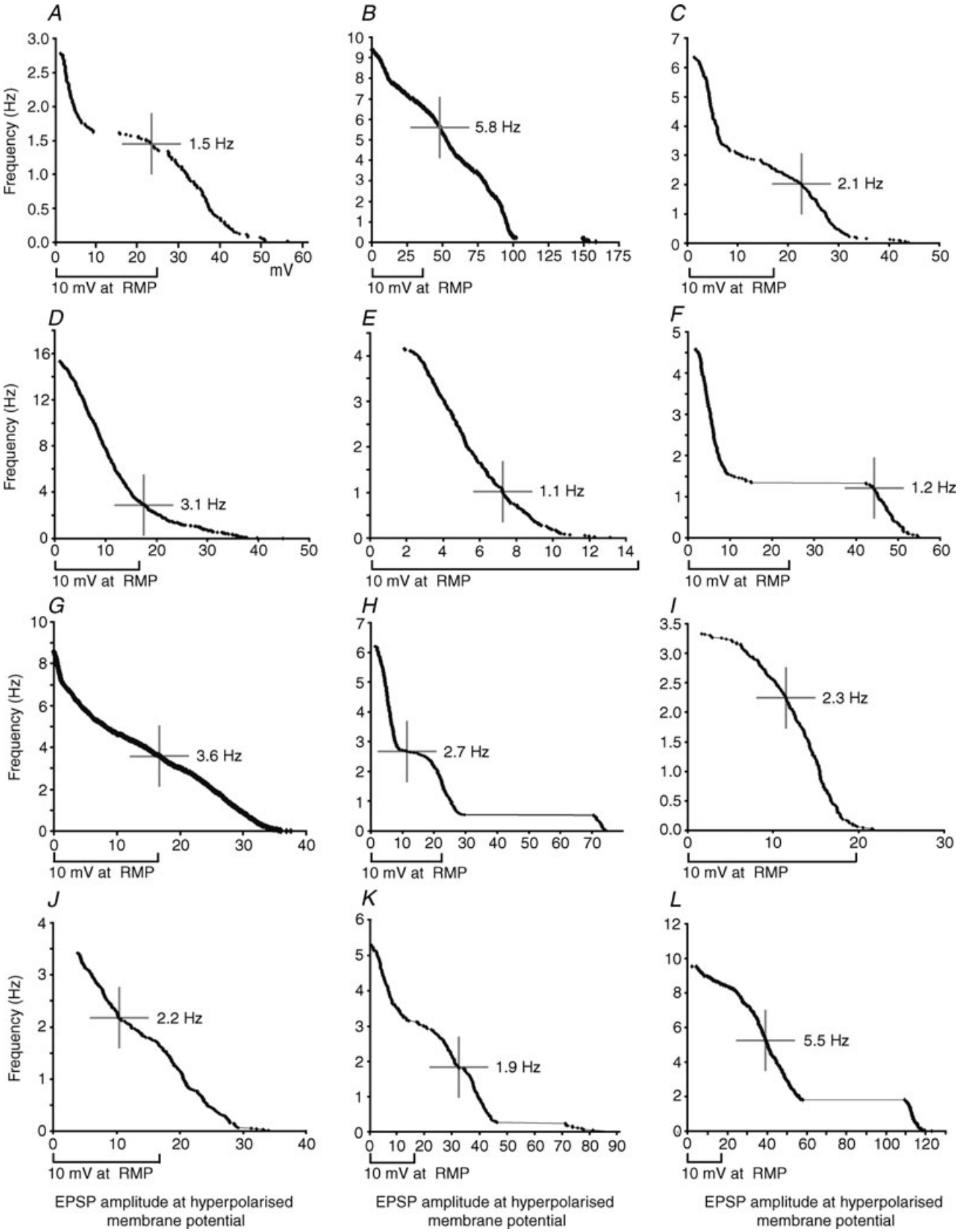

Figure 9. Cumulative frequency plots of EPSP amplitudes in relation to threshold equivalent in 12 ganglion cells

Factoring this in would lead to an adjustment of threshold equivalent to a slightly more negative value, depending on the cell's firing rate. As may be seen in Fig. 5, dominant inputs are able to fire APs less than 10 ms after a previous AP, and secondary inputs after less than 20 ms. For a typical cell firing at 3 Hz, this therefore gives us three 'dead times' of ∼15 ms each second, an error of ≤5%. As may be seen in Fig. 9, however, a downward shift in intercepts of 5% or more would make no difference to the conclusion that for most cells, threshold equivalent intersects a sloping region of the cumulative histogram of EPSP amplitudes.

Firing rates

It is not clear that there is anything intrinsically different about the physiology of preganglionic neurons providing dominant synaptic inputs compared with others. The strong cardiac rhythmicity of all inputs to the same cell – suprathreshold and subthreshold – suggests that the preganglionic neurons providing those inputs belong to the same functional class. The firing rates of dominant and secondary inputs were also similar (Fig. 7), and are in the ranges previously found for preganglionic MVC-type neurons in the cervical sympathetic trunk of rats (median 1.1 Hz, $n = 36$; Bartsch *et al.* 2000) or cats (1.11 ± 0.8 Hz; Boczek-Funcke *et al.* 1993) and the lumbar trunk of cats (1.8 ± 1.3 Hz; Jänig & Szulczyk, 1980). The frequency match between dominant and secondary inputs should be qualified by the caveat that only inputs triggering action potentials were counted, and failures would have been commoner in the secondary group. Assuming that such errors were not great, however, the present data are compatible with the view that the preganglionic neurons providing dominant inputs are not a distinct population of spinal neurons with different firing patterns: rather, one of several inputs to a ganglion cell appears to be selected and strengthened under the influence of postsynaptic factors (Ireland, 1999; McLachlan, 2003).

In most cases, postganglionic spike activity was driven from two or more preganglionic sources. It was therefore not surprising to find that the population mean firing rate of ganglion cells (2.9 Hz) was a little over double that of unitary inputs (1.4 Hz). In cells where dominant inputs were active, they accounted for 39% of spike activity, giving a post- to preganglionic activity ratio of 2.6. Together, these data indicate that an average of between two and three active preganglionic inputs were converging on each ganglion cell to determine its resting activity. Additional inputs probably contribute small EPSPs with a lower chance of reaching threshold. Finally, silent inputs – dominant and secondary – may be recruited to activity when central sympathetic drive is raised under distinct functional conditions.

Implications for the function of the ganglionic synapse

Although vasomotor ganglion cells have been considered to act as simple relays (noted above), several pieces of evidence suggest that ganglionic transmission *in vivo* may show short-term plasticity (Jänig, 2006). In a striking example, brief tetanic stimulation of a cut white ramus in anaesthetised cats was shown to enhance ongoing postganglionic MVC and CVC fibre activity (transmitted by undisturbed preganglionic connections) for tens of minutes by an action in the ganglion (Blumberg & Jänig, 1983). *In vitro*, several mechanisms have been identified that influence the excitability of sympathetic ganglion cells. Potassium channels underlying the M-current and the afterhyperpolarization may be suppressed by angiotensin II (Ma *et al.* 2006) and by muscarinic actions of acetylcholine (Adams *et al.* 1982). Chloride channels open in response to increases in intracellular sodium, causing an activity-related reduction in ganglion cell excitability (Sacchi *et al.* 2003, 2007).

While tetanic stimulation and high levels of peptides may depolarize ganglion cells sufficiently for them to generate trains of action potentials independently of any preganglionic input (Morris *et al.* 2005; Ma *et al.* 2006), it seems obvious that before this happens, substantially lower levels of the same agents would enhance the chances of peri-threshold EPSPs triggering action potentials (Kullmann & Horn, 2006). Circulating angiotensin II may be predicted to have such a modulatory action, and to enhance ganglionic transmission, but direct evidence is yet lacking. Evidence does exist for the reverse (inhibitory) action by atrial natriuretic peptide (ANP), however. Floras (1995) showed that systemic infusion of ANP reduced muscle sympathetic activity in humans, but this effect was reversed by a short-acting cholinesterase inhibitor (edrophonium): an action at sympathetic ganglia was inferred.

In summary, the present results demonstrate that the ganglionic synapse, at least in the MVC pathway,

Cumulative EPSP amplitude histograms of 12 ganglion cells (*A–L*), plotted as in Fig. 8. Cell *G* repeats Fig. 8. The original firing rate of each ganglion cell is given, next to a cross that denotes the intercepts at threshold equivalent. The abscissa in each case refers to EPSP amplitudes in the hyperpolarised membrane. To adjust these values to what they would have been at RMP, appropriate calibration brackets are given below each graph (derived as described in text). Note that threshold equivalent lies on or near a plateau of the relation in 2 cells (*F* and *H*), but on sloping sections in the remainder.

possesses considerable scope for modulation. While under resting conditions its role in synaptic integration appears limited, a role for summation of subthreshold EPSPs under different conditions has not been excluded. Most strikingly, however, the present findings demonstrate that dominant synaptic inputs are only a minor source of post-ganglionic vasomotor activity. A key role for the secondary synaptic inputs has been identified. The finding that EPSP amplitudes are distributed in a continuum straddling threshold has important functional implications: it means that ganglionic throughput will be a continuous function of cell threshold. Some of the factors that are able to modify ganglion cell threshold are noted above, but others will no doubt be identified by future work. The ganglionic synapse in this presumed vasomotor pathway thus acts not as a passive relay, but as a variable gate. The fact that it is located outside the blood–brain barrier renders this locus in the vasomotor drive pathway an attractive target for therapeutic manipulation.

References

Adams PR, Brown DA & Constanti A (1982). M-currents and other potassium currents in bullfrog sympathetic neurones. *J Physiol* **330**, 537–572.

Baron R, Jänig W & Kollmann W (1988). Sympathetic and afferent somata projecting in hindlimb nerves and the anatomical organization of the lumbar sympathetic nervous system of the rat. *J Comp Neurol* **275**, 460–468.

Bartsch T, Jänig W & Häbler HJ (2000). Reflex patterns in preganglionic sympathetic neurons projecting to the superior cervical ganglion in the rat. *Auton Neurosci* **83**, 66–74.

Blumberg H & Jänig W (1983). Enhancement of resting activity in postganglionic vasoconstrictor neurones following short-lasting repetitive activation of preganglionic axons. *Pflugers Arch* **396**, 89–94.

Boczek-Funcke A, Dembowsky K, Häbler HJ, Jänig W & Michaelis M (1993). Spontaneous activity, conduction velocity and segmental origin of different classes of thoracic preganglionic neurons projecting into the cat cervical sympathetic trunk. *J Auton Nerv Syst* **43**, 189–200.

Boczek-Funcke A, Häbler HJ, Jänig W & Michaelis M (1992). Respiratory modulation of the activity in sympathetic neurones supplying muscle, skin and pelvic organs in the cat. *J Physiol* **449**, 333–361.

Cane KN & Anderson CR (2009). Generating diversity: Mechanisms regulating the differentiation of autonomic neuron phenotypes. *Auton Neurosci* **151**, 17–29.

Floras JS (1995). Inhibitory effect of atrial natriuretic factor on sympathetic ganglionic neurotransmission in humans. *Am J Physiol Regul Integr Comp Physiol* **269**, R406–412.

Grosse M & Jänig W (1976). Vasoconstrictor and pilomotor fibres in skin nerves to the cat's tail. *Pflugers Arch* **361**, 221–229.

Häbler HJ, Jänig W, Krummel M & Peters OA (1994). Reflex patterns in postganglionic neurons supplying skin and skeletal muscle of the rat hindlimb. *J Neurophysiol* **72**, 2222–2236.

Horn JP & Stofer WD (1988). Spinal origins of preganglionic B and C neurons that innervate paravertebral sympathetic ganglia nine and ten of the bullfrog. *J Comp Neurol* **268**, 71–83.

Horn JP & Stofer WD (1989). Preganglionic and sensory origins of calcitonin gene-related peptide-like and substance P-like immunoreactivities in bullfrog sympathetic ganglia. *J Neurosci* **9**, 2543–2561.

Ireland DR (1999). Preferential formation of strong synapses during re-innervation of guinea-pig sympathetic ganglia. *J Physiol* **520**, 827–837.

Ireland DR, Davies PJ & McLachlan EM (1999). Calcium channel subtypes differ at two types of cholinergic synapse in lumbar sympathetic neurones of guinea-pigs. *J Physiol* **514**, 59–69.

Ivanov A (1991). Pattern of ongoing activity in rat superior cervical ganglion neurons projecting to a specific target. *J Auton Nerv Syst* **32**, 77–79.

Ivanov A & Purves D (1989). Ongoing electrical activity of superior cervical ganglion cells in mammals of different size. *J Comp Neurol* **284**, 398–404.

Ivanov A & Skok VI (1992). Neuronal mechanisms responsible for ongoing activity of rabbit superior cervical ganglion neurons. *J Auton Nerv Syst* **41**, 61–66.

Jänig W (1988). Pre- and postganglionic vasoconstrictor neurons: differentiation, types, and discharge properties. *Annu Rev Physiol* **50**, 525–539.

Jänig W (2006). *The Integrative Action of the Autonomic Nervous System. Neurobiology of Homeostasis*. Cambridge University Press, Cambridge.

Jänig W & Kümmel H (1981). Organization of the sympathetic innervation supplying the hairless skin of the cat's paw. *J Auton Nerv Syst* **3**, 215–230.

Jänig W & McLachlan EM (1992). Characteristics of function-specific pathways in the sympathetic nervous system. *Trends Neurosci* **15**, 475–481.

Jänig W & Szulczyk P (1980). Functional properties of lumbar preganglionic neurones. *Brain Res* **186**, 115–131.

Karila P & Horn JP (2000). Secondary nicotinic synapses on sympathetic B neurons and their putative role in ganglionic amplification of activity. *J Neurosci* **20**, 908–918.

Kubota A, Ootsuka Y, Xu T & Terui N (1995). The 10-Hz rhythm in the sympathetic nerve activity of cats, rats and rabbits. *Neurosci Lett* **196**, 173–176.

Kullmann PH & Horn JP (2006). Excitatory muscarinic modulation strengthens virtual nicotinic synapses on sympathetic neurons and thereby enhances synaptic gain. *J Neurophysiol* **96**, 3104–3113.

Li C & Horn JP (2006). Physiological classification of sympathetic neurons in the rat superior cervical ganglion. *J Neurophysiol* **95**, 187–195.

Ma X, Bielefeldt K, Tan ZY, Whiteis CA, Snitsarev V, Abboud FM & Chapleau MW (2006). Dual mechanisms of angiotensin-induced activation of mouse sympathetic neurones. *J Physiol* **573**, 45–63.

Macefield VG, Wallin BG & Vallbo AB (1994). The discharge behaviour of single vasoconstrictor motoneurones in human muscle nerves. *J Physiol* **481**, 799–809.

McLachlan EM (2003). Transmission of signals through sympathetic ganglia: modulation, integration or simply distribution? *Acta Physiol Scand* **177**, 227–235.

McLachlan EM, Davies PJ, Häbler HJ & Jamieson J (1997). On-going and reflex synaptic events in rat superior cervical ganglion cells. *J Physiol* **501**, 165–181.

McLachlan EM, Häbler HJ, Jamieson J & Davies PJ (1998). Analysis of the periodicity of synaptic events in neurones in the superior cervical ganglion of anaesthetized rats. *J Physiol* **511**, 461–478.

Morris JL, Gibbins IL & Jobling P (2005). Post-stimulus potentiation of transmission in pelvic ganglia enhances sympathetic dilatation of guinea-pig uterine artery *in vitro*. *J Physiol* **566**, 189–203.

Perkel DH, Gerstein GL & Moore GP (1967). Neuronal spike trains and stochastic point processes. I. The single spike train. *Biophys J* **7**, 391–418.

Polosa C, Schondorf R & Laskey W (1982). Stabilization of the discharge rate of sympathetic preganglionic neurons. *J Auton Nerv Syst* **5**, 45–54.

Purves D (1975). Functional and structural changes in mammalian sympathetic neurones following interruption of their axons. *J Physiol* **252**, 429–463.

Purves D, Rubin E, Snider WD & Lichtman J (1986). Relation of animal size to convergence, divergence, and neuronal number in peripheral sympathetic pathways. *J Neurosci* **6**, 158–163.

Sacchi O, Rossi ML, Canella R & Fesce R (2003). Voltage- and activity-dependent chloride conductance controls the resting status of the intact rat sympathetic neuron. *J Neurophysiol* **90**, 712–722.

Sacchi O, Rossi ML, Canella R & Fesce R (2007). Regulation of the subthreshold chloride conductance in the rat sympathetic neuron. *Eur J Neurosci* **25**, 1112–1126.

Selyanko AA, Robbins J & Brown DA (1995). Putative M-type potassium channels in neuroblastoma-glioma hybrid cells: inhibition by muscarine and bradykinin. *Receptors Channels* **3**, 147–159.

Skok VI & Ivanov AY (1983). What is the ongoing activity of sympathetic neurons? *J Auton Nerv Syst* **7**, 263–270.

Tanaka M, Ootsuka Y, McKinley MJ & McAllen RM (2007). Independent vasomotor control of rat tail and proximal hairy skin. *J Physiol* **582**, 421–433.

Tatarchenko LA, Ivanov A & Skok VI (1990). Organization of the tonically active pathways through the superior cervical ganglion of the rabbit. *J Auton Nerv Syst* **30**(Suppl), S163–168.

Wheeler DW, Kullmann PH & Horn JP (2004). Estimating use-dependent synaptic gain in autonomic ganglia by computational simulation and dynamic-clamp analysis. *J Neurophysiol* **92**, 2659–2671.

Yawo H (1989). Rectification of synaptic and acetylcholine currents in the mouse submandibular ganglion cells. *J Physiol* **417**, 307–322.

Author contributions

All experiments were performed at the Howard Florey Institute by B.B., with guidance from P.D. and further assistance from R.McA. and W.J. R.McA. and B.B. analysed the data and wrote the paper, receiving critical input from P.D. and W.J. All authors contributed to study design and data interpretation; all have approved the final manuscript.

Acknowledgements

We thank David Trevaks for technical help and the National Heart Foundation and the National Health and Medical Research Council for grant support (G02M0665 and 454494, respectively). R.McA. held an NHMRC Fellowship (277901) and W.J. received an Allen & Maria Myers Visiting Fellowship.